JACS
JOURNAL OF THE AMERICAN CHEMICAL SOCIETY

Article

pubs.acs.org/JACS

π−π Interaction Assisted Hydrodefluorination of Perfluoroarenes by Gold Hydride: A Case of Synergistic Effect on C−F Bond Activation

Hongbin Lv,[†,‡] Jin-Hui Zhan,[†,‡] Yuan-Bo Cai,[†] Yi Yu,[†] Bingwu Wang,[†] and Jun-Long Zhang*[,†]

[†]Beijing National Laboratory for Molecular Sciences, State Key Laboratory of Rare Earth Materials Chemistry and Applications, College of Chemistry and Molecular Engineering, Peking University, Beijing 100871, P. R. China

Supporting Information

ABSTRACT: "Synergistic effect" is prevalent in natural metalloenzymes in activating small molecules, and the success has inspired the development of artificial catalysts capable of unprecedented organic transformations. In this work, we found that the attractive π−π interaction between organic additives (as electron-donors) and the perfluorinated arenes (as electron acceptors) is effective in gold hydride catalyzed activation of C−F bonds, specifically hydrodefluorination (HDF) of perfluoroarenes catalyzed by the Sadighi's gold hydrides [(NHC)AuH] (NHC = N-heterocyclic carbene). Although a weak interaction between [(NHC)AuH] and perfluoroarenes was observed from ^{1}H NMR and UV−vis spectroscopies, low reactivity of [(NHC)AuH] toward HDF was found. In contrast, in the presence of *p*-*N*,*N*-dimethylaminopyridine (DMAP), the HDF of perfluoroarenes with silanes can be efficiently catalyzed by [(NHC)AuH], resulting in mainly the *para*-hydrodefluorinated products with up to 90% yield and 9 turnovers. The yield of the reaction increases with the more electron-withdrawing groups and degree of fluorination on the arenes, and the HDF reaction also tolerates different function groups (such as formyl, alkynyl, ketone, ester, and carboxylate groups), without reduction or hydrogenation of these function groups. To reveal the role of DMAP in the reactions, the possible π−π interaction between DMAP and perfluoroarenes was suggested by UV−vis spectral titrations, ^{1}H NMR spectroscopic studies, and DFT calculations. Moreover, ^{1}H and ^{19}F-NMR studies show that this π−π interaction promotes hydrogen transfer from [(NHC)AuH] to pyridyl N atom, resulting in C−F bond cleavage. The interpretation of π−π interaction assisted C−F activation is supported by the reduced activation barriers in the presence of DMAP (31.6 kcal/mol) than that in the absence of DMAP (40.8 kcal/mol) for this reaction. An analysis of the charge distribution and transition state geometries indicate that this HDF process is controlled by the π−π interaction between DMAP and perfluoroarenes, accompanied with the changes of partial atomic charges.

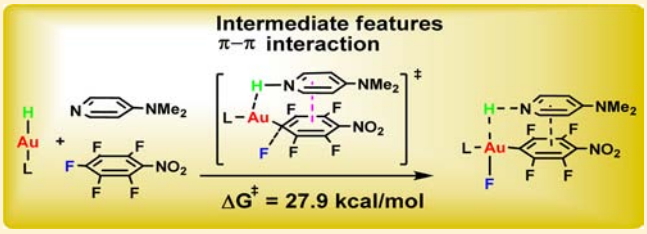

INTRODUCTION

Activation of the C−F bond by transition-metal catalysts has attracted much attention in recent years. Such an endeavor not only provides potential new routes to fluorinated organic compounds but also advances fundamental understanding of the formation of metal-fluoro complexes, which are important intermediates in the C−F bond formation reactions.[1−3] As previously demonstrated in experimental and theoretical studies, late transition metals such as Fe, Ru, Os, Co, Rh, Ir, Ni, Pd, and Pt may be preferred over early transition metals in performing catalytic functionalization of C−F bonds, because of the relatively weaker M−F bonds in late transition metals.[4−18] Therefore, it is important to explore the reactions catalyzed by later transition metals in order to enrich the repertoire of metal-catalyzed C−F bond activation. Since Sadighi, Gray, Tsui, and their co-workers pioneered the isolation of stable and active molecular gold-fluoride[19] and gold-hydride[20] supported by NHC (N-heterocyclic carbene) ligands, gold(I) complexes began to emerge as an important class of metal catalysts in C−F bond formation and activation.[21−27] The ability of gold(I) fluoride in nucleophilic fluorination of alkynes was exploited by Sadighi and co-workers,[21] which opened up a way for the application of gold fluorides as intermediates and catalysts in C−F bond formation as well as other transformations such as cross-coupling.[28−38] More recently, Toste and co-workers reported C(sp^3)−F reductive elimination from *cis*-F_2Au(III)-(R)(IPr) intermediates, which were generated by oxidation of (IPr)AuR complexes with XeF_2.[39] In contrast to tremendous progress made in the gold-fluoride system, reports of application of gold-hydrides in organofluorine chemistry are rare, even though metal hydrides are also important in C−F bond activations.[11,40−53] While gold(I) complexes containing Xantphos type ligands have been shown to catalyze the hydrodefluorination (HDF) of perfluoroarenes efficiently, it has been difficult to isolate a stable and reactive gold hydride.[54,55] Instead, we observed only binuclear "Au_2H" species with μ-H as a bridge, which is not active toward HDF. In this work, we turn our attention to Sadighi's gold hydride, the sole monomeric terminal gold hydride supported by NHC ligands,[20] as a starting point in exploring C−F bond activation by gold hydride complexes.

Received: May 29, 2012
Published: September 17, 2012

dx.doi.org/10.1021/ja305204y | J. Am. Chem. Soc. 2012, 134, 16216−16227

Scheme 1. 'Synergistic Effect' in Transition-Metal-Catalyzed C−F Bond Activation

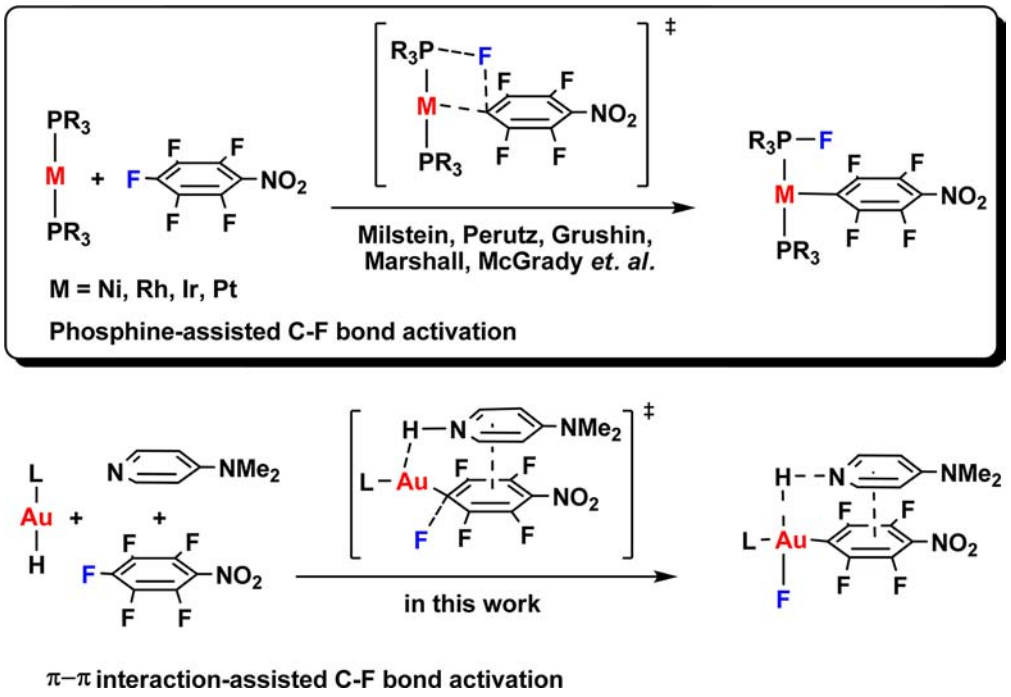

In addition to the efforts in discovering new metal catalysts, exploring appropriate organic additives to enhance the reactivity and selectivity is also important, because the additives may facilitate stabilization of transition states or activation of the substrates. Such a synergistic effect between metal active sites and/or the surrounding amino acid residues is prevalent in natural metalloenzymes, which has inspired the design and synthesis of complexes with similar combination of metal and organic additives capable of unprecedented organic transformation.[56−61] In metal-catalyzed C−F bond activation, an elegant example is "phosphine-assisted C−F bond activation" by metallophosphoranes (inset of Scheme 1).[16,62−65] Milstein and co-workers first reported $[IrMe(PEt_3)_3]$,[66] in which a phosphorus center of metal-phosphine complexes facilitated the transfer of fluorine from C−F bonds to form a fluorophosphine. This synergistic effect has been intensively studied in catalytic systems such as $[Pt(PR_3)_2]$,[67,68] $[RhF(PPh_3)_3]$,[69,70] and $[Ni(PR_3)_2]$[71,72] by Perutz, Grushin, Marshall, McGrady, and others. Although different pathways varied with the metals have been proposed for different metal catalyst systems,[73−75] the "phosphine-assisted C−F bond activation" represents a new mechanistic possibility and provides a novel route to C−F bond activation. C−F bond activation assisted by other functional groups or ligands includes stoichiometric cyclometalation by Co,[76,77] Fe,[78] and Pt[79] directed by *ortho*-chelating groups. Built upon these successes, it is important to expand the functionality of organic components and to further utilize "synergistic effect" to explore a new pathway to activate C−F bonds.

In this work, we investigated the reactivity of gold hydrides [(NHC)AuH] (NHC = IMes, IMes = *N*,*N*′-bis(2,4,6-trimethylphenyl)imidazolin-2-ylidene) toward catalytic HDF of perfluoroarenes. We indeed observed the weak interaction between [(NHC)AuH] and perfluoroarenes from ^{1}H NMR and UV−vis spectroscopies; however, no HDF occurred. Through computational studies, we found that a high activation barrier (40.8 kcal/mol) needs to be overcome if only gold hydride [(NHC)AuH] was used. More importantly, when the strong electron donating *p*-*N*,*N*-dimethylaminopyridine (DMAP) was introduced, [(IMes)AuH] exhibited much higher reactivity and the reaction became catalytic (TON = 9) with silanes as hydrogen sources. ^{1}H, ^{19}F NMR, and UV−vis spectra revealed that the formation of $\pi-\pi$ stacking intermediate between PFNB (pentafluoronitrobenzene) and DMAP is critical to the activation of the C−F bond and transfer of a hydrogen atom from gold hydrides. DFT studies pertained to the reaction processes involving $\pi-\pi$ interaction between [(IMes)AuH], DMAP, and PFNB, which is in accordance with the experimental observation. The interpretation of $\pi-\pi$ interaction-induced synergistic effect is also supported by the reduced activation barriers computed with three-component "[(NHC)AuH]+ DMAP + perfluoroarenes" and the higher barriers found with less electron donating pyridines. Based on these results, we propose a new pathway for intermolecular C−F bond activation, termed "$\pi-\pi$ interaction-assisted C−F bond activation" (Scheme 1). Such a discovery further demonstrates that the power of synergistic effect plays a central role in organometallic reactivity.

RESULTS AND DISCUSSION

Following Tsui and Sadighi's method,[20] we prepared stable gold hydrides such as [(IPr)AuH] (IPr = *N*,*N*′-bis(2,6-diisopropylphenyl)imidazolin-2-ylidene) and [(IMes)AuH] (IMes = *N*,*N*′-bis(2,4,6-trimethylphenyl)imidazolin-2-ylidene). We chose pentafluoronitrobenzene (PFNB) as a substrate to optimize the reaction conditions (Table 1), because the electron-withdrawing property of nitro group lowers the energy of the π^* orbital and makes the C−F bond more susceptible to be activated.[80] No reaction between PFNB and [(IMes)AuH] or [(IPr)AuH] was observed when stoichiometric amounts of the reactants were used (Table 1, entries 1 and 2). Addition of Et_3SiH (triethylsilane) resulted in 2,3,5,6-tetrafluoronitrobenzene in low yields, with [(IPr)AuH] exhibiting less reactivity (14% yield, Table 1, entry 4) than [(IMes)AuH] (18% yield, Table 1, entry 3). When gold(I) chlorides such as [(IMes)-

dx.doi.org/10.1021/ja305204y | J. Am. Chem. Soc. 2012, 134, 16216−16227

Table 1. Reaction Optimization for Hydrodefluorination of PFNB with Different Additives[a]

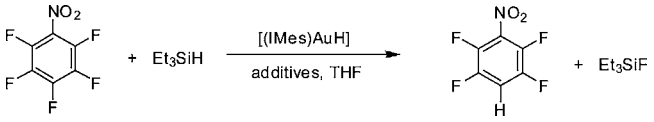

entry	catalysts (%)	additives[b]	yields (%)[c]
1[d]	[(IMes)AuH](50)	-	0
2[d]	[(IPr)AuH](50)	-	0
3	[(IMes)AuH](50)	-	18
4	[(IPr)AuH](50)	-	14
5	[(IMes)AuCl](50)	-	0
6	[(PPh_3)AuCl](50)	-	0
7	[(IMes)AuH](50)	DMAP	90
8	-	DMAP	0
9[e]	[(IMes)AuH](100)	DMAP	47
10	[(IMes)AuH](50)	$PhNMe_2$	0
11	[(IMes)AuH](50)	N-MePy	0
12	[(IMes)AuH](50)	NMP	15
13	[(IMes)AuH](50)	Cs_2CO_3	0

[a]Reaction conditions: PFNB (0.02 mmol), Et_3SiH (0.04 mmol), additive (0.02 mmol), THF (1 mL) at 40 °C for 12 h under nitrogen. The reaction was monitored by GC-MS. [b]Amounts of additives were based on gold complex. [c]Yields were determined by integration of ^{19}F NMR resonances in the product mixture (versus external or/and internal trifluoromethylbenzene) after workup based on PFNB. [d]The reaction condition is the same as that in footnote [a] but in the absence of Et_3SiH. [e]The reaction condition is the same as that in footnote [a] but in the absence of Et_3SiH.

AuCl] and [Au(PPh_3)Cl] were used to replace [(IMes)AuH], no hydrodefluorinated product was obtained (Table 1, entries 5 and 6). In cases when hydrodefluorination did occur (Table1, entries 3 and 4), no nitro group reduction product was observed under these conditions. Optimization of the reactions by varying silanes and solvents was performed, and the results were shown in Table S1 and Table S2, respectively.

To improve the efficiency of the reactions, we chose several bases such as DMAP, $PhNMe_2$ (*N*,*N*-dimethylphenylamine), N-MePy (*N*-methylpyrrole), or NMP (*N*-methyl-2-pyrrolidone), and the results are shown in entries 7−13 in Table 1. Surprisingly, when DMAP was used as an additive, PFNB was converted into 2,3,5,6-tetrafluoronitrobenzene by [(IMes)-AuH] in 90% yield (Table 1, entry 7). Control experiment showed that, in the absence of [(IMes)AuH], DMAP/Et_3SiH could not hydrodefluorinate PFNB (entry 8). Without Et_3SiH, 2,3,5,6-tetrafluoronitrobenzene was obtained in the yield of 47% with 100% [(IMes)AuH] /DMAP (Table 1, entry 9). Other bases were not effective, resulting in low yields of 0−15% (Table 1, entries 10−13). These results suggest that DMAP may not act only as a base.

A notable feature of fluorinated molecules is their electron-deficient property, due to fluorine's strong electron-withdrawing ability. This feature renders perfluoroarenes as good electron acceptors in supramolecular chemistry, through $\pi-\pi$ interaction with electron donors.[81] As previously reported, interaction between electron-rich low valent transition metals and electron-deficient perfluoroarenes is important for the oxidative addition of aromatic C−F bonds.[72,82−87] Therefore, we envisioned that the attractive $\pi-\pi$ interaction between the organic additives (as electron donors) and fluorinated arenes (as electron acceptors) may be effective for inducing new synergistic effect in activation of aromatic C−F bonds.

Since DMAP is a good electron donor and can form a $\pi-\pi$ stacking complex with electron deficient PFNB, we hypothesized that this $\pi-\pi$ interaction between DMAP and PFNB might be important in C−F bond activation. Thus, we first examined the electronic effect of pyridines with various substituents at *para*-position (*p*-CF_3, *p*-H, *p*-^{t}Bu, *p*-Me, *p*-OMe, and *p*-pyrrolidine), and the results are shown in Table 2.

Table 2. Electronic Effect of Additives on HDF of PFNB[a]

entry	additives	yield (%)[b]	pK_a of additives[c]
1	*p*-*N*,*N*-dimethylaminopyridine	90	17.95
2	*p*-pyrrolidinepyridine	40	18.33
3	*p*-methoxypyridine	14	14.23
4	*p*-*tert*-butylpyridine	6	
5	*p*-methylpyridine	6	
6	pyridine	7	12.53
7	*p*-trifluoromethylpyridine	2	
8	$PhNMe_2$	0	11.43
9	NEt_3	10	18.82
10	DBU	23	24.34

[a]The reaction was carried out with gold complex (0.01 mmol), PFNB (0.10 mmol), pyridine derivatives (0.05 mmol), and $HSiEt_3$ (0.04 mmol) in DCM at 40 °C for 12 h under nitrogen. DBU: 1,8-diazabicycloundec-7-ene. [b]Yields were determined by integration of ^{19}F NMR resonances in the product mixture (versus external or/and internal trifluoromethylbenzene) after workup based on PFNB. [c]pK_a values in MeCN were citied from Kaljurand, I.; Kütt, A.; Sooväli, L.; Rodima, T.; Mäemets, V.; Leito, I.; Koppel, I. A. *J. Org. Chem.* **2005**, *70*, 1019−1028.

Indeed, the efficiency of HDF of PFNB was found to be related to the electron donating ability of *para*-substituents on pyridines. DMAP and *p*-pyrrolidine pyridine with more electron-donating groups afforded higher yields (90 and 40%, respectively, Table 2, entries 1 and 2) whereas other pyridines with less electron-donating groups gave lower yields (Table 2, entries 3−7). We also used strong bases, such as DBU (pK_a = 24.34) and NEt_3 (pK_a = 18.82), which could not have $\pi-\pi$ interaction with PFNB, as additives. The yields of HDF of PFNB were 23% and 10%, lower than that using DMAP (pK_a = 17.95). Plotting the relationship between the yields of products and the pK_a values of the bases (Figure 1) demonstrated that the yields were not systematically dependent on the pK_a values of bases. Therefore, DMAP played the dual roles: not only as a base but also as an electron donor for $\pi-\pi$ interaction.

We also found that the ratio of PFNB to DMAP is important for the catalytic cycle. As shown in Table S3, when the amount of [(IMes)AuH] was decreased to 10 mol %, increasing the concentration of DMAP from 5 to 12.5 mM resulted in an increase of TON from 1.6 to 9 (Table S3, entries 1−3). When the concentration of DMAP is higher than 12.5 mM, lower TONs and the formation of a yellow precipitate were observed (Table S3, entries 4 and 5). Plotting yields of HDF products vs reaction time, shown in Figure 2, illustrated the critical role of DMAP in catalytic HDF of PFNB by [(IMes)AuH]. We found that gold catalysts deactivated after 12 h, and some black gold(0) precipitates appeared according to our previous report. For the changes of gold complexes, from the ^1H NMR, we observed the disappearance of gold hydride. We also used ESI-MS spectroscopy to characterize the possible metal containing species *in situ*. From the ESI-MS spectrum, we found that metal

dx.doi.org/10.1021/ja305204y | *J. Am. Chem. Soc.* 2012, 134, 16216−16227

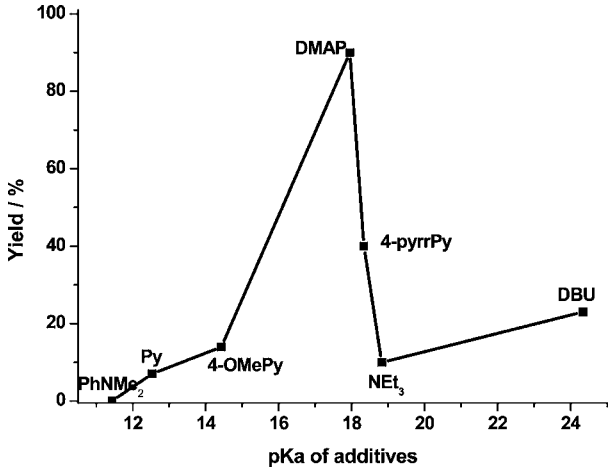

Figure 1. Relationship of yield of PFNB and pK_a values of additives.

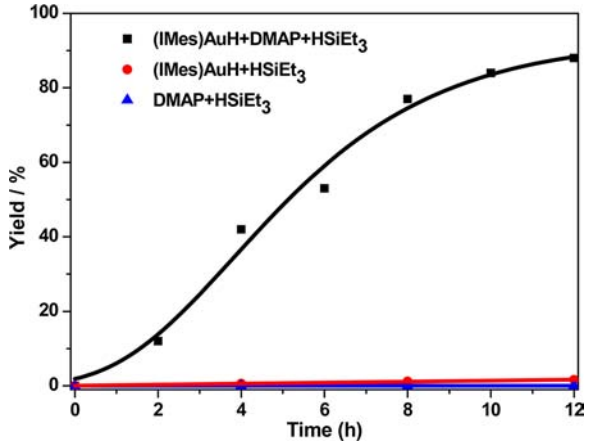

Figure 2. Time course for the HDF of PFNB (DCM, 40 °C, N_2) by 10 mol % [(IMes)AuH] in the presence of 50 mol % DMAP and 400 mol % $HSiEt_3$ (black solid box), without DMAP (red circle), without [(IMes)AuH] (blue up-facing triangle).

species such as AuL_2 (L = NHC), Au_2L_2, Au_2L_3, and Au_3L_3 (see Figure S12 in the Supporting Information), which might be the precursors for gold(0) precipitates.

Scope of Substrates. Scope of substrates was investigated using 10 mol % [(IMes)AuH], and the results are summarized in Table 3. As shown in **10**–**13**, when one fluoro atom of the hexafluorobenzene was substituted by a strong electron withdrawing group such as NO_2 (**10**), CHO (**11**), CN (**12**), and CF_3 (**13**), the HDF products (**10**–**13**) were obtained in high yields (85–90%). However, when H (**14**), F (**15**), or electron donating MeO (**16**) groups were present, no reaction occurred. This suggests that the reactivity is highly dependent on the electronic states of perfluoroarenes. The inactivity of C_6F_6 (**15**) toward this reaction is probably due to the higher energy of the LUMO of C_6F_6 than C_6F_5R (R = NO_2 **10**, CHO **11**, CN **12**, CF_3 **13**),[88] making the activation of C_6F_6 harder than C_6F_5R (**10**–**13**). Interestingly, in the presence of different functional groups such as formyl (**11**), alkynyl (**17**), ketone (**18**), ester (**19**), and carboxylate (**20**) groups, only *para* HDF products were observed, and no reduction or hydrogenation of the function groups was detected, suggesting high tolerance of different functional groups by this reaction. When pentafluoropyridine **21** was used as a substrate, the *para*-HDF product was obtained in high yield (90%), indicating that the nitrogen atom in **21** cannot coordinate to gold and the *ortho* C–F bond is not activated.[71,89] Less fluorinated substrates such as tetra- (**22**), trifluorinated nitrobenzene (**23**), and tetrafluorobenzaldehyde (**24**) resulted in *para*-HDF products with the decreased reactivity, in comparison to the perfluoro analogues, suggesting that the degree of fluorination also affects the HDF reactions.

Mechanistic Studies. Although the monomeric gold(I) hydrides containing NHC ligands are stable against exposure to air and moisture in the solid state, the moderate reactivity toward dimethyl acetylenedicarboxylate and ethyl diazoacetate has been observed by Sadighi and co-workers.[20] More importantly, the featured hydride signal of [(IMes)AuH] (3.43 ppm, CD_2Cl_2) is sensitive to the coordination environment of the gold atom, which provides an opportunity to monitor the changes of [(IMes)AuH] using the ^{1}H NMR techniques.

1. Interaction between [(IMes)AuH] and PFNB. Although the reaction of [(IMes)AuH] and PFNB did not afford the HDF product, surprisingly, we observed the upfield chemical shift of the hydride signal from 3.43 to 3.26 ppm in ^{1}H NMR (Figure 3a). Other protons of [(IMes)AuH] changed less than 0.02 ppm (Figure S1), suggesting the weak interaction between gold hydride and PFNB. To exclude the possibility of the hydride interacting with the nitro group of PFNB, we used perfluorotoluene to replace PFNB. Similar upfield shift of the signal of the hydride was detected (Figure 3b), although the chemical shift ($\Delta\delta_{CF3}$ vs $\Delta\delta_{NO2}$: −0.07 vs −0.17 ppm, Figure 3b) was smaller. A further monitor of the kinetic process of such interactions (Figure 3c) showed that the PFNB interacted with [(IMes)AuH] much faster than perfluorotoluene. Therefore, we conclude that the weak interaction between [(IMes)-AuH] and perfluoroarenes depends on the electronic effect of perfluoroarenes.

The interaction between [(IMes)AuH] and PFNB was further studied by UV–vis spectroscopy. As shown in Figure 4a, a new broad absorption band with its maximum at 400 nm was observed when [(IMes)AuH] and PFNB were mixed, and such a band was absent in solution containing either [(IMes)AuH] or PFNB alone.

To elucidate the interaction between [Au–H] (**1**) and PFNB, we used the DFT method through B3LYP functional (the Stuttgart-Dresden (SDD) pseudopotential and associated basis set for Au, implemented in the Gaussian 09 package). As shown in Figure 5, the lowest unoccupied molecular orbital (LUMO) of complex **2** is localized mainly in the π^* orbital of PFNB, and the highest occupied molecular orbital (HOMO) comes mainly from the Au–H σ bond, which interacts slightly with the π orbital of PFNB. The energies of HOMO (−5.91 eV) and LUMO (−2.30 eV) of complex **2** are higher than those for PFNB (−7.75 eV for HOMO and −2.90 eV for LUMO) and lower than those for [Au–H] (−5.57 eV for HOMO and −0.43 eV for LUMO), respectively. Moreover, the NBO (Natural Bond Orbitals) charge analysis based on the optimized structures indicates that the charge of hydride (H1) changes from −0.26 *e* ([Au–H] **1**) to −0.30 *e* in complex **2**. The increasing negative charge of the hydride atom is consistent with the upfield shift of the hydride signal in the ^{1}H NMR spectra. Similar NBO analysis of the interaction between [Au–H] and perfluorotoluene showed that the charge of hydride changed from −0.26 *e* to −0.28 *e*, indicating a weaker interaction in this complex, again consistent with smaller upfield shift of the hydride signal in the ^{1}H NMR spectra of the complex between [Au–H] and perfluorotoluene.

dx.doi.org/10.1021/ja305204y | J. Am. Chem. Soc. 2012, 134, 16216–16227

Table 3. Hydrodefluorination of Different Fluoroarenes Mediated by [(IMes)AuH]

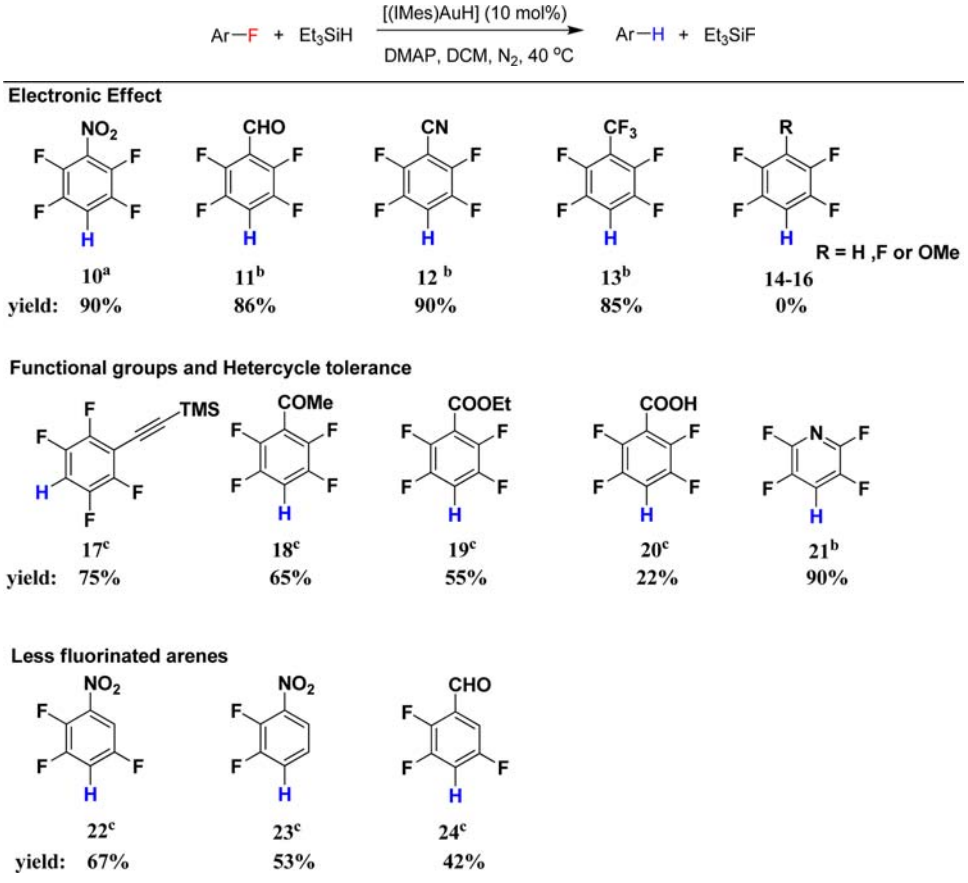

[a]The reaction was carried out with gold complex (2.5 mM), PFNB (25 mM), DMAP (12.5 mM), and $HSiEt_3$ (100 mM) in DCM at 40 °C for 12 h under nitrogen. [b]DMAP (50 mM) was added. [c]DMAP (100 mM) was added.

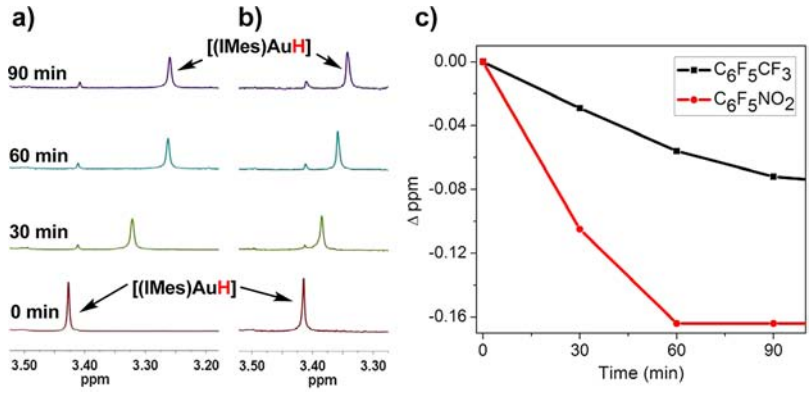

Figure 3. (a) and (b) ^{1}H NMR spectra for gold hydride mixing with PFNB (1 equiv) and perfluorotoluene (1 equiv), respectively. Red for [(IMes)AuH], green, cyan, and purple for 30, 60, and 90 min, respectively, after addition of substrates to [(IMes)AuH] in CD_2Cl_2. (c) Time course plots for the changes of chemical shifts between [(IMes)AuH] and PFNB or perfluorotoluene.

Encouraged by these results, the DFT calculation of electronic excitation spectra was carried out, and the results were shown in Figure 4b, in which the lowest excited states (S1) of three systems were marked, respectively. A new absorption band at 399 nm was found in complex **2**, which corresponds to the electronic transition from HOMO to LUMO. Moreover, the molecular orbital analysis shows that HOMO is dominated by [(IMes)AuH] (92.8%) and LUMO is dominated by PFNB (99.6%). Thus, the appearance of the new absorption band at 399 nm is due to the weak interaction between [(IMes)AuH] and PFNB. The combined ^{1}H NMR, UV−vis experiments, and theoretical studies all demonstrated the weak interaction between [(NHC)AuH] and PFNB or perfluorotoluene.

2. Effect of DMAP on the Interaction between [(IMes)AuH] and PFNB. To elucidate the role of DMAP, we first investigated the interaction between [(IMes)AuH] and DMAP. From ^{1}H NMR spectrum, we could not observe any changes of proton or hydride signals when mixing [(IMes)AuH] and DMAP, indicating no interaction between [(IMes)AuH] and DMAP (Figure S2).

dx.doi.org/10.1021/ja305204y | J. Am. Chem. Soc. 2012, 134, 16216−16227

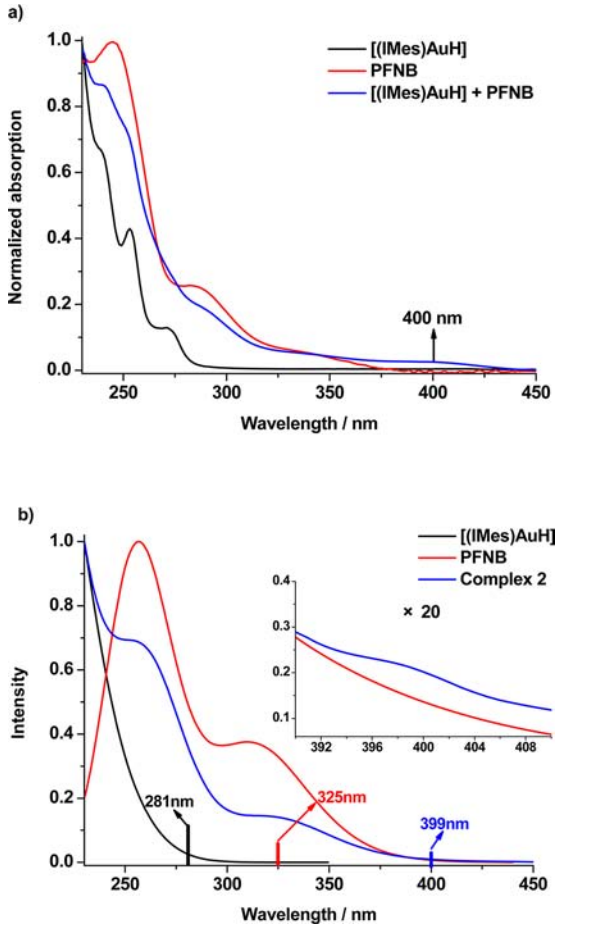

Figure 4. (a) UV absorption of [(IMes)AuH] (black), PFNB (red), and a 1:1 mixture of [(IMes)AuH] and PFNB (blue) [c] = 1.2×10^{-5} M. (b) Electronic excitation spectra of [(IMes)AuH] (black), PFNB (red), and complex **2** (blue) calculated by TDDFT and B3LYP/SDD/6-31G(d). The oscillator strength is given as the height of the peak. The lowest energy state was marked by vertical bar.

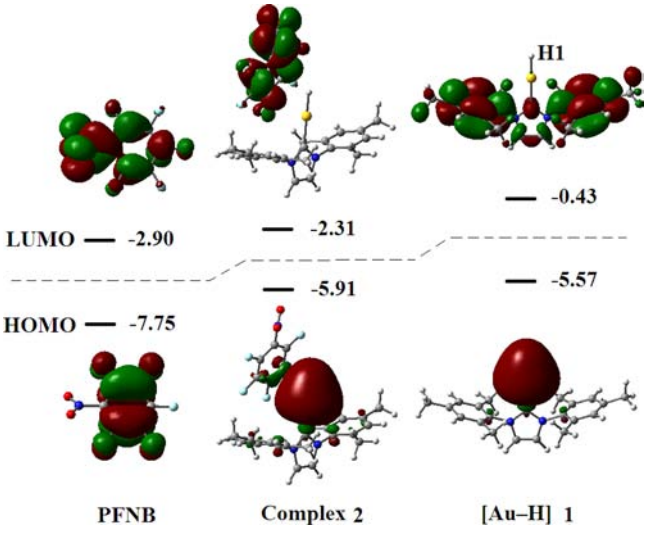

Figure 5. Calculated HOMOs and LUMOs of PFNB, [Au–H], and complex **2**. The orbital energies were shown in eV.

Since HDF of PFNB is highly dependent on the electron donating ability of *para*-substituents on pyridines (Table 2), we considered the interaction between *para*-substituted pyridines and PFNB. UV–vis spectroscopic studies showed that a new broad absorption band centered at 413 nm appeared when PFNB was added to the THF solution of DMAP (Figure S3). When DMAP was replaced by other pyridines with different *para*-substituents such as Me, ^{t}Bu, and MeO, new broad bands with maximum absorptions at 475, 474, and 468 nm, respectively, were observed (Table S4). For *p*-CF_3Pyridine, no obvious new absorption formed. According to previous studies, these new absorptions may be assigned to charge transfer between pyridines and PFNB.[90] However, we observed that the formation of charge transfer bands were kinetic and measured the k_2 values as shown in Table S5. These k_2 values decreased with decreasing of the electron-donating ability of the *para*-substituted groups. For the charge transfer is a very rapid process (electron transfer) and occurs upon efficient overlap of π orbitals of a donor and an acceptor, these slow processes of formation of charge transfer bands may be due to the different orientation or a change in geometry of pyridines.

We have also studied the ^{1}H NMR signal of $\pi-\pi$ stacking complex between pyridine bases and PFNB. When DMAP and PFNB (1:1) were mixed in CD_2Cl_2 (Figure 6a(i)), the protons of DMAP downfield shifted from 8.25 to 9.06 ppm and 6.46 to 6.98 ppm, respectively. This downfield shift of protons of DMAP was due to $\pi-\pi$ interaction between DMAP and PFNB, which causes deshielding of the protons. The different *para*-substituents of pyridines affect the $\pi-\pi$ interaction with PFNB. For example, although similarly downfield shifts (from 8.44 to 8.57–9.45 and from 6.83 to 7.39–7.56 ppm) of protons of pyridines were observed in the mixture of *p*-methoxypyridine and PFNB; however, the signal of *p*-methoxypyridine disappeared slowly even after 2 days (Figure S4).

Interaction between PFNB and DMAP gave an insoluble yellow precipitate of 4-onio-substituted 2,3,5,6-tetrafluoronitrobenzene[91,92] if the mixture is left for 1 h, and this precipitate did not react with [(IMes)AuH]. We used ^{1}H NMR to monitor the reaction process, and the aromatic region of ^{1}H NMR spectra was shown in Figure 6a. When 1 equiv of DMAP was added to the solution of [(IMes)AuH] and PFNB (1:1) in CD_2Cl_2, three new signals at 6.85, 7.88, and 15.33 ppm appeared while the hydride signal (δ = 3.43 ppm) disappeared (see Figure 6a(ii)). The new peaks at 7.88 and 6.85 ppm are doublet, assignable to DMAP, indicating that [(IMes)AuH] participates in the $\pi-\pi$ interaction between DMAP and PFNB and a new intermediate forms. Interestingly, the new proton signal at 15.33 ppm at downfield is similar to that of NH^+ in pyridinium trifluorosulfonate in CD_2Cl_2 (16.18 ppm, Figure S5). When [(IMes)AuD] is used to replace [(IMes)AuH], only the proton signal at 15.33 ppm disappears, suggesting the proton at 15.33 ppm is from the hydride of [(IMes)AuH] (Figure S6). More interestingly, we observed a new F signal at −248.61 ppm in ^{19}F NMR spectra (Figure 6b), which is identical to Au–F signal of [(IMes)AuF].[19,21] To confirm this assignment, we added 1 equiv of $HSiEt_3$ to this solution and observed the formation of Et_3SiF (F signal at −176.01 ppm). These results demonstrated that the addition of DMAP to [(IMes)AuH] and PFNB resulted in transferring the proton from [(IMes)AuH] to DMAP, accompanied by the formation of Au–F intermediate.

To understand the effect of [(IMes)AuH] on the interaction between PFNB and DMAP, we have also undertaken DFT calculations. First, we obtained a bound complex **3** between DMAP and PFNB through the B3LYP functional (Figure S7). The HOMO is mainly localized at DMAP, while the LUMO is

dx.doi.org/10.1021/ja305204y | J. Am. Chem. Soc. 2012, 134, 16216–16227

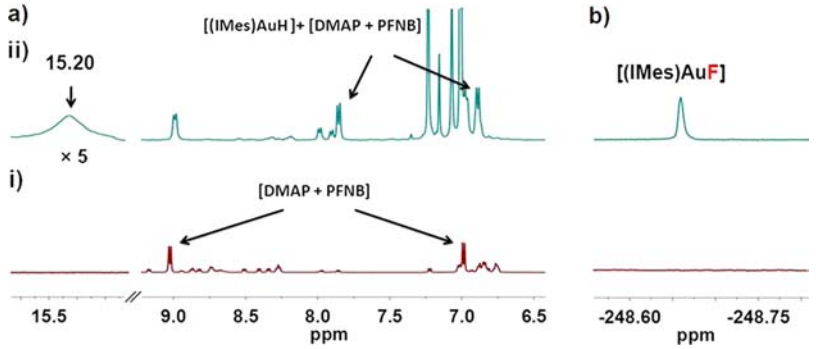

Figure 6. Cyan line for (a) ^{1}H NMR and (b) ^{19}F NMR spectra for addition of DMAP (1 equiv) to the mixed solution of [(IMes)AuH] (1 equiv) and PFNB (1equiv) in CD_2Cl_2; red line for (a) ^{1}H NMR and (b) ^{19}F NMR spectra of mixture of DMAP (1 equiv) and PFNB (1 equiv) in CD_2Cl_2.

localized at PFNB. The aromatic rings are parallel and adapt a "face-to-face" orientation with the inclined angle of two aromatic rings as 8.7°. Based on complex **3**, we added [(IMes)AuH] and optimized a loosely bound complex **4**. As shown in Figure S7, the "face-to-face" orientation between PFNB and DMAP is interrupted because of the interaction between [(IMes)AuH] and PFNB. The angle between the two aromatic rings is hinged to 45.1°, and the distance of the N atom of DMAP and the *para*-C atom of PFNB increased from 3.94 Å in complex **3** to 6.19 Å in complex **4**, preventing the nucleophilic attack of *p*-F of PFNB by the pyridyl N atom.

To account for the protonation of DMAP, we postulate that the proton transfer from [(IMes)AuH] to DMAP is assisted by PFNB (Figure 7). This possible transformation is considered to

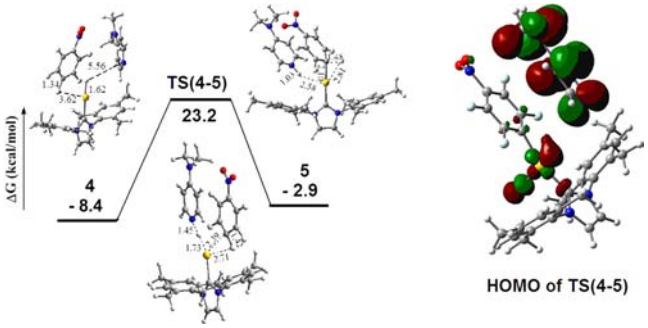

Figure 7. The transition state geometry of hydrogen transfer **TS(4−5)** and molecular orbitals.

involve a loosely bound complex **4** to the protonated DMAP intermediate **5**, proceeding through a transition state **TS(4−5)**. The structure of **TS(4−5)** features the "face-to-face" orientation between PFNB and DMAP, and this orientation is suitable for the $\pi-\pi$ interaction. In **TS(4−5)**, the C−F bond is weakened by the interaction between C, F, and Au atoms and elongated from 1.34 to 1.42 Å. The highest occupied molecular orbital HOMO of **TS(4−5)** shows a striking feature for the interaction between the σ bond of Au−H and the *p*-orbital of the N atom of DMAP. Along the pathway, the intermediate **5** is located, in which the N−H bond is shortened to 1.03 Å, resulting in the protonation of DMAP.

Moreover, NBO charge analysis reveals atomic charge distribution in **TS(4−5)**. As shown in Figure 8a, the charge for DMAP and PFNB in **TS(4−5)** is 0.22 *e* and −0.68 *e*, suggesting the $\pi-\pi$ interaction between the electron donor DMAP and the electron acceptor PFNB. NBO charge density analysis suggests that the hydride in initial complex **4** turns to a

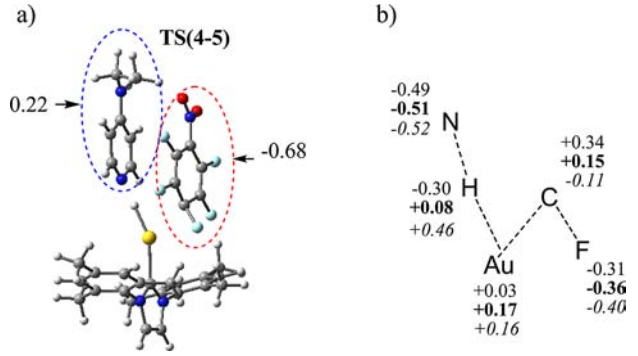

Figure 8. (a) The charge for DMAP and PFNB in **TS(4−5)**. (b) Computed natural atomic charges for precomplex **4** (plain text), **TS(4−5)** (bold), and intermediate **5** (italics) for the proton transfer process in the first step of DMAP-assisted catalytic reaction.

proton in intermediate **5**, according to the changes of the electronic charge on hydrogen atom (−0.30, +0.08, and +0.46 *e*, Figure 8b). In this step, the charges of Au and the hydride turn more positive, while N, C, and F atoms become more negative, indicating that the C−F bond is activated and elongated as the result of charge repulsion in the C−F bond.

To better understand the effect of DMAP, DFT calculations were performed on the transition states of the proton transfer process with *para*-pyridine derivatives with different electronic effects (*p*-methoxy, *p*-methyl, and *p*-trifluoromethyl). Free energies of these transition states have been calculated and summarized in Figure S8. With the decrease of the electron-donating ability of the *para*-substituents (DMAP, *p*-methoxypyridine, *p*-methylpyridine, and *p*-trifluoromethylpyridine), the energies of transition states increase to 23.2, 27.7, 28.7, and 31.5 kcal/mol, respectively, in consistence with the experimental results shown in Table 2.

Proposed Mechanism for C−F Bond Activation by [(IMes)AuH]. Based on the above experimental and theoretical studies for C−F bond activation mediated by [(IMes)AuH] (**a**), we propose the following mechanism as depicted in Scheme 2. In the absence of DMAP (path I), [(IMes)AuH] interacts with PFNB first, forming complex **b**, which is supported by ^{1}H NMR experiments (Figure 3) and UV−vis spectra (Figure 4a) and theoretical studies (Figure 5). Then, the C−F bond is activated *via* the oxidative addition step to the gold(I) complex, resulting in the formation of gold(III)-fluoride complex **f**. Subsequent reduction elimination leads to the product and gold(I)-fluoride complex **e**, which reacts with silane to reform [(IMes)AuH] *via* H/F exchange. In the

dx.doi.org/10.1021/ja305204y | J. Am. Chem. Soc. 2012, 134, 16216−16227

Scheme 2. Calculated Mechanism I (in the Absence of DMAP) and Mechanism II (DMAP-Assisted) for the Hydrodefluorination of Fluoroarenes Mediated by [(IMes)AuH]

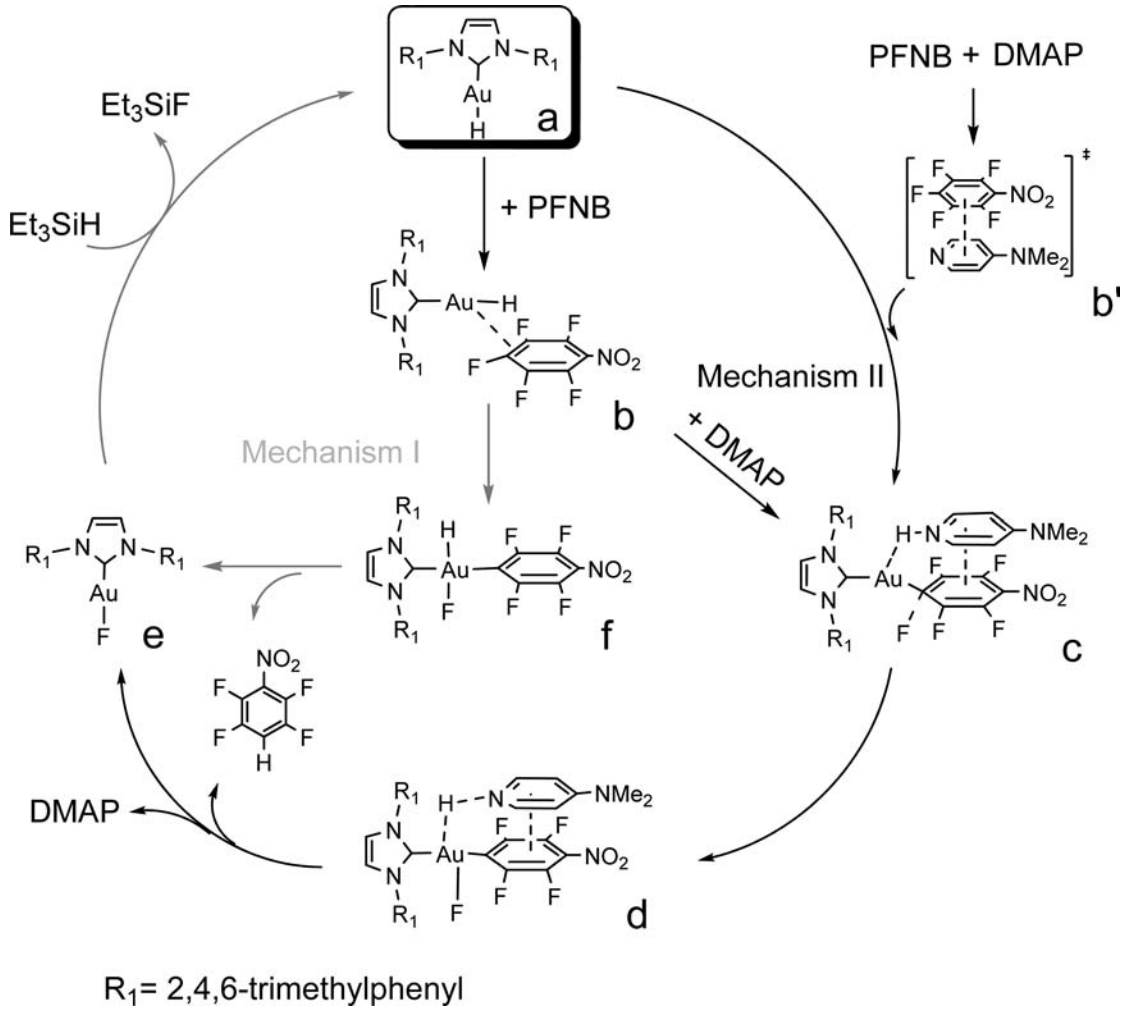

presence of DMAP (path II), we assumed that the interaction among [(IMes)AuH], DMAP, and PFNB would occur *via* two possible pathways, either complex **b** interacts with DMAP or [(IMes)AuH] interacted with the $\pi-\pi$ stacking complex of DMAP and PFNB (complex **b**′). In either case, the generation of protonated DMAP complex **c** is postulated to be the key step. Then the oxidative addition reaction of the C−F bond to gold(I) occurs in the complex **c**, affording the DMAP involved gold(III) complex **d**. Subsequent reductive elimination results in formation of the product and the complex **e**.

Computed Reaction Profiles for HDF by [(IMes)AuH]. To define alternative pathways whether in the absence or presence of DMAP,[85,93,94] calculation has been done with the full system [(IMes)AuH] using the Gaussian 09 package,[95] only with $HSiEt_3$ being simplified as $HSiMe_3$.

1. Path I: In the Absence of DMAP. The computed geometries and relative free energies of the stationary points during the process are shown in Figure 9. In the first step, a loosely bound adduct **2** is formed (ΔG = −4.7 kcal/mol) in which the geometries of gold hydride [Au−H] **1** and PFNB are barely perturbed from their separated structures. The C−F bond activation can then be initialized from complex **2**, and a three-centered transition state **TS(2−6)** (ΔG = 36.1 kcal/mol) is located. In **TS(2−6)**, the C−F bond is weakened and stretched to 1.65 Å, and a new Au−C bond (2.17 Å) is formed.

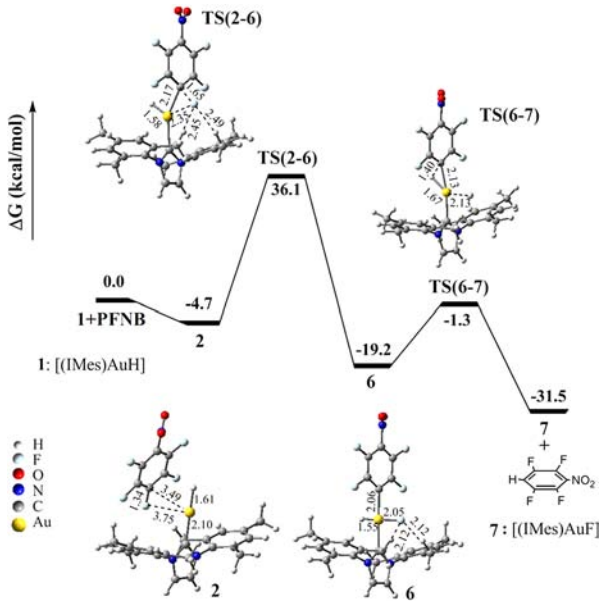

Figure 9. Computed geometries (with selected key distances in Å) and free energy surface for the pathway I (in the absence of DMAP).

dx.doi.org/10.1021/ja305204y | *J. Am. Chem. Soc.* 2012, 134, 16216−16227

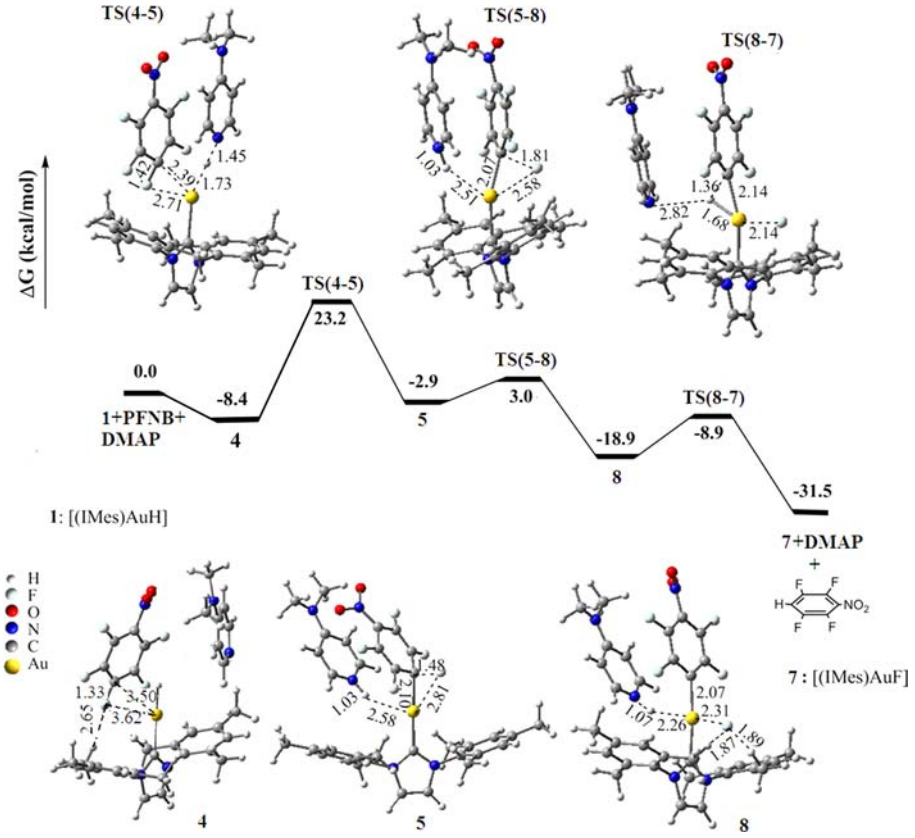

Figure 10. Computed geometries (with selected key distances in Å) and free energy surface for the DMAP-assisted pathway.

The *para*-F atom is twisted relative to the aromatic plane of PFNB by 54° and stabilized by gold and H atom of ligand. Consequently, the planar tetra-coordinated gold(III) fluoride intermediate **6** is formed. Therefore, it is a direct oxidative addition process, which has been previously reported in C−F bond activations by d^{10} metals such as Ni and Pt.[10]

The [(IMes)AuF] intermediate **7** and $(C_5F_4NO_2)$C−H product are subsequently formed *via* a transition state **TS(6−7)** with a free energy barrier of 17.9 kcal/mol. This is a reductive elimination and exothermic process (12.3 kcal/mol). In **TS(6−7)**, the Au(III)−H bond is elongated to 1.67 Å and then cleaved to form Au(I)−F intermediate **7** and C−H product, coupled with the elongation (2.13 Å in **TS(6−7)** vs 2.06 Å in **6**) and cleavage of the Au−C bond.

2. Path II: In the Presence of DMAP. As shown in Figure 10, starting from the weakly bound complex **2**, DMAP reacts with complex **2** and forms complex **4**. Along the pathway, complex **4** transforms into the intermediate **5**, through proton transfer from [Au−H] to DMAP *via* **TS(4−5)** (ΔG = 23.2 kcal/mol). In the intermediate **5**, DMAP is protonated, and the Au−C bond between Au(I) ion and PFNB is formed. The Au(I) ion is linearly coordinated by carbon with the distance of the Au−C bond 2.10 Å, and the C−F bond elongates to 1.48 Å, compared with the 1.34 Å in complex **4**, indicating that the C−F bond is activated. Then, gold(I) inserts into the C−F bond *via* a transition state **TS(5−8)** and Au(III)-F intermediate **8** is produced. In **TS(5−8)** (ΔG = 5.9 kcal/mol), the C−F bond is further elongated to 1.81 Å, and the distance between gold and fluorine atoms is shortened from 2.81 to 2.58 Å. Finally, the intermediate **8** converts to DMAP, Au(I)−F intermediate **7** and product through a hydrogen transfer transition state **TS(8−7)** (ΔG = 5.9 kcal/mol). In **TS(8−7)**, the distance of the N−H bond is elongated to 2.82 Å, in comparison to that in intermediate **8** (1.07 Å), accompanied with the shortened distance of the C−H bond (1.36 Å).

According to a reviewer's suggestion, we tried to explore the possibility of HF reductive elimination from intermediate **5**. First, if HF is formed, it will be captured by DMAP to form an ammonium hydrofluoride. In intermediate **5** the atoms of proton, Au, C, and F are almost coplanar, with the H and F atoms being located on both sides of the Au−C bond, and the distance between H and F is 4.42 Å. Therefore, direct HF reductive elimination from intermediate **5** is very difficult. We failed to find the transition state from intermediate **5** to an HF intermediate through rotating the C−F structure to make F accessible to H atom. Second, an intermediate structure **9** of HF reductive elimination according to related work by Macgregor, Whittlesey, and their co-workers[96] is optimized as shown in Figure S11. After the optimization of the intermediate structure, the free energy of intermediate **9** is −63.3 kcal/mol, which is much lower than that of the final products with Au(I)−F intermediate **7**, DMAP, and product (ΔG = −31.5 kcal/mol). Combined with the experimental results that the Au(I)-F intermediate **7** was observed by ^{19}F NMR (Figure 6) but there was no HF complex observed in experiments, we conclude that, from intermediate **5**, there might be other pathways to intermediate **7** but not the HF reductive elimination.

The overall calculated potential energy surface for **Path I** indicates that the Au(I) inserting into the C−F bond is the rate-limiting step of the tandem reaction and the activation free energy for the tandem reaction is 40.8 kcal/mol. For **Path II**, the highest energy barrier corresponds to hydrogen transfer and thus becomes the rate-determining step of the catalytic cycle.

dx.doi.org/10.1021/ja305204y | J. Am. Chem. Soc. 2012, 134, 16216−16227

The activation free energy in this pathway is 31.6 kcal/mol, which is much lower than that of **Path I** (40.8 kcal/mol). Because the difference between **Path I** and **Path II** is the presence of DMAP, these calculations clearly show that the participation of DMAP in the reaction makes the C−F bond activation more accessible; such computational results strongly support the experimental observations that the DMAP-assisted process can occur under the mild condition and in high yields.

■ CONCLUSIONS

In summary, we have demonstrated the first example of unusual $\pi-\pi$ interaction assisted C−F bond activation by gold(I) hydrides. Although direct HDF of fluoroaromatics could not be achieved by [(IMes)AuH] due to its low reactivity, the addition of DMAP can effectively promote the reaction process. Through mechanistic studies, we have observed the weak interaction between [(NHC)AuH] and perfluoroarenes by ^{1}H NMR and UV−vis spectroscopies; however, this interaction is not efficient to perform C−F activation through oxidative addition or nucleophilic attack of the C−F bond. More importantly, we have observed that the formation of an intermediate between PFNB and DMAP though $\pi-\pi$ interaction could promote the transfer of proton in [(NHC)-AuH], accompanied by C−F bond activation.

Density functional calculations have been used to model possible mechanisms for this unusual C−F bond activation reaction between PFNB and [(NHC)AuH] in the presence or absence of DMAP. The calculations provide a reasonable framework to guide our understanding of the reaction mechanism involving key steps such as the weak interaction between [(IMes)AuH] and PFNB, $\pi-\pi$ interaction-assisted C−F bond activation, and [Au−F] intermediate formation. The key points that emerge from the calculations are as follows: (i) the C−F bond activation is the rate-determining step with the highest activation barrier among the entire energy profiles for HDF reactions. The calculated pathways show that the energy barriers for C−F bond cleavage by [Au−H] is much higher (8.4 kcal/mol) than that in the presence of DMAP. (ii) Formation of an intermediate between DMAP and PFNB through $\pi-\pi$ interaction allows charge redistribution and the hydride could transform from hydridic to protonic, while the initially positively charged carbon that loses the F atom turns neutral and then carbon ionic.[97] Hydrogen atom transfers from gold hydride to PFNB through the formation of pyridinium ion, indicating that DMAP also plays a role as a base.

Overall, using stable gold hydride [(NHC)AuH] to initialize C−F bond activation for hydrodefluorination of fluoroarenes demonstrated the potential application of gold complexes and made gold catalysts appealing in the context of C−F bond activation and functionalization of fluorocarbons. It is not surprising to observe the low reactivity of [(IMes)AuH] during the catalytic reactions because it is very stable and comparatively chemically inert. However, this unusual $\pi-\pi$ interaction-assisted C−F bond activation represents a further mechanistic possibility for the activation of C−F bonds by transition metals and may be important for future design of effective ligands to support electron-rich metal centers.

■ EXPERIMENTAL SECTION

General Synthetic Methods. Unless otherwise stated, all reactions were performed under nitrogen atmosphere in a dried reaction flask using glovebox or standard Schlenk techniques. Dry, oxygen-free solvents were used throughout. Dichloromethane was dried by heating at reflux with calcium hydride. THF and benzene were distilled over sodium under a nitrogen atmosphere. Commercially available reagents were used without further purification. Deuterium solvents were stored with 4 Å molecular sieves.

UV−vis spectra were recorded on an Agilent 8453 UV−vis spectrophotometer equipped with an Agilent 89090A thermostat (±0.1 °C). GC/MS spectra were recorded on an Agilent 7890A GC system/5975c mass spectrometer using electron impact source. IR spectra were recorded on a Nicolet ECTOR22 FT-IR spectrometer as KBr pellets. Elemental analyses were performed on Elementar Vario MICRO CUBE. ^{1}H and ^{19}F NMR spectra were recorded on a Bruker 400 MHz instrument at 293 K. All chemical shifts were reported in ppm, and all coupling constants were in Hz. For ^{19}F NMR spectra, benzotrifluoride was used as the internal reference at −63.0 ppm.

External Standard Methods. An NMR tube was filled with gold catalyst (2.5 mM), fluoroarenes (25 mM), silanes (100 mM) in DCM, and a standardized capillary tube of benzotrifluoride was inserted. An initial ^{19}F spectrum was recorded at room temperature. The capillary was removed from NMR tube, and the reaction mixture was heated at oil bath at 313 K for 12 h. The NMR tube was removed from oil bath and cooled, and the capillary was reinserted before further ^{19}F spectra were periodically recorded. HDF products were integrated relative to the standard to get turnover numbers.

Time Course Plot of HDF of PFNB in the Presence of DMAP. [(IMes)AuH] (2.5 mM), PFNB (25 mM), DMAP (12.5 mM), $HSiEt_3$ (100 mM), and benzotrifluoride (10 mM, internal standard) were mixed in CD_2Cl_2 in a Teflon sealed NMR tube. The NMR tube was heated at 40 °C, and the ^{19}F NMR monitoring was performed every 2 h. The yield of HDF product was calculated by the integration of ^{19}F NMR resonances of product relative to that of internal standard.

UV−Vis Study of $\pi-\pi$ Interaction of DMAP with PFNB. To the DMAP solution (concentration was 1.7×10^{-4} M), 20, 40, 60, 80, 100 equiv of PFNB was added. UV spectra were collected every 30 s; k_{obs} was simulated as first-order reaction ($A = A_0 \times (1\text{-}e^{(-k_{obs} \times t)})$, A: absorbance), according to the intensity change of absorption at 413 nm which was assigned as charge-transfer band.

UV−Vis Study of $\pi-\pi$ Interactions of *para*-Substituted Pyridines with Pentafluoronitrobenzene. To the *para*-substituted pyridine solution (concentration was 1.7×10^{-3} M), 20, 40, 60, 80, 100 equiv of PFNB was added. UV−vis absorption spectra were recorded in 4 days, while the k_{obs} was simulated according to the intensity change at maximum absorption. k_2 was calculated by linear fitting of k_{obs} with equivalent of PFNB toward pyridines.

NMR Study of Interaction between [(IMes)AuH] and Perfluoroarenes. [(IMes)AuH] (2.5 mg) was dissolved in CD_2Cl_2 (0.5 mL) in a Teflon sealed NMR tube; then 1.10 mg of PFNB or perfluorotoluene was added via syringe under Ar. The chemical shifts of protons of [(IMes)AuH] after addition of PFNB were detected every 30 min by ^{1}H NMR as shown in Figure S1.

NMR Study of Effect of DMAP on the Interaction between [(IMes)AuH] and PFNB. [(IMes)AuH] (2.5 mg) and PFNB (1.10 mg) were dissolved in CD_2Cl_2 (0.5 mL) in a Teflon sealed NMR tube; then DMAP (0.5 mg) was added under Ar in a glovebox. Formation of intermediate with proton transfer from [(IMes)AuH] to DMAP was detected by ^{1}H NMR, and the formation of HDF product and [(IMes)AuF] was confirmed by ^{19}F NMR.

Computational Studies. All calculations were carried out with the Gaussian 09 package. Unless otherwise stated, the geometry optimization of the stationary points was performed using B3LYP hybrid functional with the 6-31G** basis set for the main group atoms and the SDD pseudopotential[98] and associated basis set for gold. The vibrational frequency calculations at the same level were carried out to confirm each stationary point to be either a minimum or transition state (TS). In several cases where TS are not easily confirmed by animation of their vibrations, intrinsic reaction coordinate (IRC) paths were calculated to connect each TS to corresponding reactant and product. The single point energies were also calculated using the MP2 method with the 6-311+G** basis set for C, N, F, O Si, and H and SDD for Au. Gibbs free energies (G) were also calculated and used in the following discussions. To keep the computational study efficient,

dx.doi.org/10.1021/ja305204y | J. Am. Chem. Soc. 2012, 134, 16216−16227

the experimentally used triethylsilane (Et_3SiH) was replaced by Me_3SiH.

■ ASSOCIATED CONTENT

Supporting Information

The optimization of gold-hydride catalyzed hydrodefluorination of perfluoroarenes; spectra for mechanistic studies; and the coordinates of the DFT-optimized intermediates and transition states. This material is available free of charge via the Internet at http://pubs.acs.org.

■ AUTHOR INFORMATION

Corresponding Author

zhangjunlong@pku.edu.cn.

Author Contributions

‡These authors contributed equally.

Notes

The authors declare no competing financial interest.

■ ACKNOWLEDGMENTS

This project was supported by National Key Basic Research Support Foundation of China (NKBRSFC) (2010CB912302) and the National Scientific Foundation of China (grant no. 20971007).

■ REFERENCES

(1) *Inorganic Fluorine Chemistry: Toward the 21st Century*; Thrasher, J. S., Strauss, S. H., Eds.; ACS Editions: Washington, DC, 1994.

(2) *Organofluorine Compounds: Chemistry and Application*; Hiyama, T., Kanie, K., Kusumoto, T., Morizawa, Y., Shimizu, M., Eds.; Springer-Verlag: Berlin, 2000.

(3) *Organofluorine Chemistry*; Uneyama, K., Ed.; Blackwell: Oxford, U.K., 2006.

(4) Kiplinger, J. L.; Richmond, T. G.; Osterberg, C. E. *Chem. Rev.* **1994**, *94*, 373−431.

(5) *Activation of Carbon-Fluorine Bonds by Oxidative Addition to Low-Valent Transition Metals*; Osterberg, C. E., Richmond, T. G., Eds.; American Chemical Society: Washington, DC, 1994.

(6) Burdeniuc, J.; Jedlicka, B.; Crabtree, R. H. *Chem. Ber./Recl.* **1997**, *130*, 145−154.

(7) Plenio, H. *Chem. Rev.* **1997**, *97*, 3363−3384.

(8) Murphy, E. F.; Murugavel, R.; Roesky, H. W. *Chem. Rev.* **1997**, *97*, 3425−3468.

(9) Richmond, T. G. *Angew. Chem., Int. Ed.* **2000**, *39*, 3241−3244.

(10) Braun, T.; Perutz, R. N. *Chem. Commun.* **2002**, 2749−2757.

(11) Torrens, H. *Coord. Chem. Rev.* **2005**, *249*, 1957−1985.

(12) *Transition-Metal Mediated C-F Bond Activation*; Perutz, R. N., Braun, T., Eds.; Elsevier: Amsterdam, The Netherlands, 2007; Vol. *1*.

(13) Guihaume, J.; Clot, E.; Eisenstein, O.; Perutz, R. N. *Dalton Trans.* **2010**, *39*, 10510−10519.

(14) Sun, A. D.; Love, J. A. *Dalton Trans.* **2010**, *39*, 10362−10374.

(15) Yanai, H.; Taguchi, T. *Eur. J. Org. Chem.* **2011**, 5939−5954.

(16) Clot, E.; Eisenstein, O.; Jasim, N.; Macgregor, S. A.; McGrady, J. E.; Perutz, R. N. *Acc. Chem. Res.* **2011**, *44*, 333−348.

(17) Braun, T.; Wehmeier, F. *Eur. J. Inorg. Chem.* **2011**, 613−625.

(18) Klahn, M.; Rosenthal, U. *Organometallics* **2012**, *31*, 1235−1244.

(19) Laitar, D. S.; Muller, P.; Gray, T. G.; Sadighi, J. P. *Organometallics* **2005**, *24*, 4503−4505.

(20) Tsui, E. Y.; Muller, P.; Sadighi, J. P. *Angew. Chem., Int. Ed.* **2008**, *47*, 8937−8940.

(21) Akana, J. A.; Bhattacharyya, K. X.; Muller, P.; Sadighi, J. P. *J. Am. Chem. Soc.* **2007**, *129*, 7736−7737.

(22) Schuler, M.; Silva, F.; Bobbio, C.; Tessier, A.; Gouverneur, V. *Angew. Chem., Int. Ed.* **2008**, *47*, 7927−7930.

(23) Gorske, B. C.; Mbofana, C. T.; Miller, S. J. *Org. Lett.* **2009**, *11*, 4318−4321.

(24) de Haro, T.; Nevado, C. *Adv. Synth. Catal.* **2010**, *352*, 2767−2772.

(25) Wang, W. B.; Jasinski, J.; Hammond, G. B.; Xu, B. *Angew. Chem., Int. Ed.* **2010**, *49*, 7247−7252.

(26) Mankad, N. P.; Toste, F. D. *J. Am. Chem. Soc.* **2010**, *132*, 12859−12861.

(27) de Haro, T.; Nevado, C. *Chem. Commun.* **2011**, *47*, 248−249.

(28) Peng, Y.; Cui, L.; Zhang, G. Z.; Zhang, L. M. *J. Am. Chem. Soc.* **2009**, *131*, 5062−5063.

(29) Zhang, G. Z.; Peng, Y.; Cui, L.; Zhang, L. M. *Angew. Chem., Int. Ed.* **2009**, *48*, 3112−3115.

(30) Brenzovich, W. E.; Benitez, D.; Lackner, A. D.; Shunatona, H. P.; Tkatchouk, E.; Goddard, W. A.; Toste, F. D. *Angew. Chem., Int. Ed.* **2010**, *49*, 5519−5522.

(31) Melhado, A. D.; Brenzovich, W. E.; Lackner, A. D.; Toste, F. D. *J. Am. Chem. Soc.* **2010**, *132*, 8885−8887.

(32) Brenzovich, W. E.; Brazeau, J. F.; Toste, F. D. *Org. Lett.* **2010**, *12*, 4728−4731.

(33) Ball, L. T.; Green, M.; Lloyd-Jones, G. C.; Russell, C. A. *Org. Lett.* **2010**, *12*, 4724−4727.

(34) Zhang, G. Z.; Luo, Y. D.; Wang, Y. Z.; Zhang, L. M. *Angew. Chem., Int. Ed.* **2011**, *50*, 4450−4454.

(35) Qian, J. Q.; Liu, Y. K.; Zhu, J.; Jiang, B.; Xu, Z. Y. *Org. Lett.* **2011**, *13*, 4220−4223.

(36) Stavber, S. *Molecules* **2011**, *16*, 6432−6464.

(37) Tkatchouk, E.; Mankad, N. P.; Benitez, D.; Goddard, W. A.; Toste, F. D. *J. Am. Chem. Soc.* **2011**, *133*, 14293−14300.

(38) Liu, L. P.; Hammond, G. B. *Chem. Soc. Rev.* **2012**, *41*, 3129−3139.

(39) Mankad, N. P.; Toste, F. D. *Chem. Sci.* **2012**, *3*, 72−76.

(40) Belt, S. T.; Helliwell, M.; Jones, W. D.; Partridge, M. G.; Perutz, R. N. *J. Am. Chem. Soc.* **1993**, *115*, 1429−1440.

(41) Aizenberg, M.; Milstein, D. *Science* **1994**, *265*, 359−361.

(42) Aizenberg, M.; Milstein, D. *J. Am. Chem. Soc.* **1995**, *117*, 8674−8675.

(43) Edelbach, B. L.; Jones, W. D. *J. Am. Chem. Soc.* **1997**, *119*, 7734−7742.

(44) Edelbach, B. L.; Rahman, A. K. F.; Lachicotte, R. J.; Jones, W. D. *Organometallics* **1999**, *18*, 3170−3177.

(45) Jasim, N. A.; Perutz, R. N. *J. Am. Chem. Soc.* **2000**, *122*, 8685−8693.

(46) Kraft, B. M.; Jones, W. D. *J. Organomet. Chem.* **2002**, *658*, 132−140.

(47) Jones, W. D. *Dalton Trans.* **2003**, 3991−3995.

(48) Clot, E.; Megret, C.; Kraft, B. M.; Eisenstein, O.; Jones, W. D. *J. Am. Chem. Soc.* **2004**, *126*, 5647−5653.

(49) Vela, J.; Smith, J. M.; Yu, Y.; Ketterer, N. A.; Flaschenriem, C. J.; Lachicotte, R. J.; Holland, P. L. *J. Am. Chem. Soc.* **2005**, *127*, 7857−7870.

(50) Rieth, R. D.; Brennessel, W. W.; Jones, W. D. *Eur. J. Inorg. Chem.* **2007**, 2839−2847.

(51) Whittlesey, M. K.; Reade, S. P.; Mahon, M. F. *J. Am. Chem. Soc.* **2009**, *131*, 1847−1861.

(52) Kuhnel, M. F.; Lentz, D. *Angew. Chem., Int. Ed.* **2010**, *49*, 2933−2936.

(53) Kraft, B. M.; Clot, E.; Eisenstein, O.; Brennessel, W. W.; Jones, W. D. *J. Fluorine Chem.* **2010**, *131*, 1122−1132.

(54) Ito, H.; Takagi, K.; Miyahara, T.; Sawamura, M. *Org. Lett.* **2005**, *7*, 3001−3004.

(55) Zhan, J.-H.; Lv, H.; Yu, Y.; Zhang, J.-L. *Adv. Synth. Catal.* **2012**, *354*, 1529−1541.

(56) Paull, D. H.; Abraham, C. J.; Scerba, M. T.; Alden-Danforth, E.; Lectka, T. *Acc. Chem. Res.* **2008**, *41*, 655−663.

(57) Denes, F.; Perez-Luna, A.; Chemla, F. *Chem. Rev.* **2010**, *110*, 2366−2447.

(58) Rueping, M.; Koenigs, R. M.; Atodiresei, I. *Chem.—Eur. J.* **2010**, *16*, 9350−9365.

(59) Marcelli, T.; Hiemstra, H. *Synthesis-Stuttgart* **2010**, 1229−1279.

(60) Stegbauer, L.; Sladojevich, F.; Dixon, D. J. *Chem. Sci.* **2012**, *3*, 942−958.
(61) Allen, A. E.; MacMillan, D. W. C. *Chem. Sci.* **2012**, *3*, 633−658.
(62) Uneyama, K.; Amii, H. *J. Fluorine Chem.* **2002**, *114*, 127−131.
(63) Mazurek, U.; Schwarz, H. *Chem. Commun.* **2003**, 1321−1326.
(64) Amii, H.; Uneyama, K. *Chem. Rev.* **2009**, *109*, 2119−2183.
(65) Goodman, J.; Macgregor, S. A. *Coord. Chem. Rev.* **2010**, *254*, 1295−1306.
(66) Blum, O.; Frolow, F.; Milstein, D. *J. Chem. Soc., Chem. Commun.* **1991**, 258−259.
(67) Jasim, N. A.; Perutz, R. N.; Whitwood, A. C.; Braun, T.; Izundu, J.; Neumann, B.; Rothfeld, S.; Stammler, H. G. *Organometallics* **2004**, *23*, 6140−6149.
(68) Nova, A.; Erhardt, S.; Jasim, N. A.; Perutz, R. N.; Macgregor, S. A.; McGrady, J. E.; Whitwood, A. C. *J. Am. Chem. Soc.* **2008**, *130*, 15499−15511.
(69) Grushin, V. V.; Marshall, W. J. *J. Am. Chem. Soc.* **2004**, *126*, 3068−3069.
(70) Macgregor, S. A.; Roe, D. C.; Marshall, W. J.; Bloch, K. M.; Bakhmutov, V. I.; Grushin, V. V. *J. Am. Chem. Soc.* **2005**, *127*, 15304−15321.
(71) Nova, A.; Reinhold, M.; Perutz, R. N.; Macgregor, S. A.; McGrady, J. E. *Organometallics* **2010**, *29*, 1824−1831.
(72) Hatnean, J. A.; Johnson, S. A. *Organometallics* **2012**, *31*, 1361−1373.
(73) Macgregor, S. A. *Chem. Soc. Rev.* **2007**, *36*, 67−76.
(74) Macgregor, S. A.; Wondimagegn, T. *Organometallics* **2007**, *26*, 1143−1149.
(75) Erhardt, S.; Macgregor, S. A. *J. Am. Chem. Soc.* **2008**, *130*, 15490−15498.
(76) Arisawa, M.; Suzuki, T.; Ishikawa, T.; Yamaguchi, M. *J. Am. Chem. Soc.* **2008**, *130*, 12214−12215.
(77) Mendoza, C.; Bernes, S.; Torrens, H.; Arroyo, M. *Organometallics* **2010**, *29*, 2646−2659.
(78) Xu, X. F.; Sun, H. J.; Shi, Y. J.; Jia, J.; Li, X. Y. *Dalton Trans.* **2011**, *40*, 7866−7872.
(79) Crespo, M. *Organometallics* **2012**, *31*, 1216−1234.
(80) Langer, J.; Dabkowska, I.; Zhang, Y.; Illenberger, E. *Phys. Chem. Chem. Phys.* **2008**, *10*, 1523−1531.
(81) Reichenbacher, K.; Suss, H. I.; Hulliger, J. *Chem. Soc. Rev.* **2005**, *34*, 22−30.
(82) Bach, I.; Porschke, K. R.; Goddard, R.; Kopiske, C.; Kruger, C.; Rufinska, A.; Seevogel, K. *Organometallics* **1996**, *15*, 4959−4966.
(83) Braun, T.; Cronin, L.; Higgitt, C. L.; McGrady, J. E.; Perutz, R. N.; Reinhold, M. *New J. Chem.* **2001**, *25*, 19−21.
(84) Reinhold, M.; McGrady, J. E.; Perutz, R. N. *J. Am. Chem. Soc.* **2004**, *126*, 5268−5276.
(85) Schaub, T.; Fischer, P.; Steffen, A.; Braun, T.; Radius, U.; Mix, A. *J. Am. Chem. Soc.* **2008**, *130*, 9304−9317.
(86) Johnson, S. A.; Taylor, E. T.; Cruise, S. J. *Organometallics* **2009**, *28*, 3842−3855.
(87) Johnson, S. A.; Mroz, N. M.; Valdizon, R.; Murray, S. *Organometallics* **2011**, *30*, 441−457.
(88) Dillow, G. W.; Kebarle, P. *J. Am. Chem. Soc.* **1989**, *111*, 5592−5596.
(89) Cronin, L.; Higgitt, C. L.; Karch, R.; Perutz, R. N. *Organometallics* **1997**, *16*, 4920−4928.
(90) Rabie, U. M. *Collect. Czech. Chem. Commun.* **2006**, *71*, 1359−1370.
(91) Murray, C. B.; Sandford, G.; Korn, S. R.; Yufit, D. S.; Howard, J. A. K. *J. Fluorine Chem.* **2005**, *126*, 571−576.
(92) Schmidt, A.; Mordhorst, T.; Namyslo, J. C.; Telle, W. *J. Heterocycl. Chem.* **2007**, *44*, 679−684.
(93) Braun, T.; Foxon, S. P.; Perutz, R. N.; Walton, P. H. *Angew. Chem., Int. Ed.* **1999**, *38*, 3326−3329.
(94) Sladek, M. I.; Braun, T.; Neumann, B.; Stammler, H. G. *J. Chem. Soc., Dalton Trans.* **2002**, 297−299.
(95) Frisch, M. J. et al. *Gaussian 09, revision A.02*; Gaussian Inc.: Wallingford, CT, 2009. The complete reference is shown in the Supporting Information.
(96) Panetier, J. A.; Macgregor, S. A.; Whittlesey, M. K. *Angew. Chem., Int. Ed.* **2011**, *50*, 2783−2786.
(97) Pintado-Alba, A.; de la Riva, H.; Nieuwhuyzen, M.; Bautista, D.; Raithby, P. R.; Sparkes, H. A.; Teat, S. J.; Lopez-de-Luzuriaga, J. M.; Lagunas, M. C. *Dalton Trans.* **2004**, 3459−3467.
(98) Andrae, D.; Häussermann, U.; Dolg, M.; Stoll, H.; Preuss, H. *Theor. Chim. Acta* **1990**, *77*, 123−141.